Role of $D^*_{(s)}$ and their contributions in $B_{(s)} \to D_{(s)}hh'$ decays

Jian Chai,[1,*] Shan Cheng [ORCID],[1,2,†] and Wen-Fei Wang [ORCID][3,4,‡]

[1]*School of Physics and Electronics, Hunan University, 410082 Changsha, China*
[2]*School for Theoretical Physics, Hunan University, 410082 Changsha, China*
[3]*Institute of Theoretical Physics, Shanxi University, 030006 Taiyuan, China*
[4]*State Key Laboratory of Quantum Optics and Quantum Optics Devices,*
Shanxi University, 030006 Taiyuan, China

We demonstrate the role of $D^*_{(s)}$ and their contributions in the quasi-two-body decays $B_{(s)} \to D_{(s)}hh'$ ($h, h' = \{\pi, K\}$) in the perturbative QCD approach, stemming from the quark flavor changing $\bar{b} \to \bar{c}q_2\bar{q}_1$ and $\bar{b} \to c\bar{q}_1\bar{q}_2$ with $q_1, q_2 = \{s/d, u\}$. The main motivation of this study is the measurement of significant derivations from the simple phase-space model in the channels $B_{(s)} \to D_{(s)}hh'$ at B factories and LHC, which are now clarified as the Breit-Wigner-tail effects from the corresponding intermediate resonant states $D^*_{(s)}$. We confirm that these effects from D^* are small ($\sim 5\%$) in the quasi-two-body $B_{(s)} \to D\pi\pi(K)$ decaying channels and predict the tiny ($< 1\%$) contributions from D^* in the $B_{(s)} \to D_s K\pi(K)$ decaying channels. Our result that the $B_s \to DK\pi(K)$ decaying channel contributions were only from the Breit-Wigner-tail effect of D^*_s is in agreement with the current LHCb measurement. We recommend that the Belle-II and the LHCb Collaborations restudy the processes $B^+ \to \bar{D}^{*0}\pi^+(K^+) \to D^-\pi^+\pi^+(K^+)$ to reveal the structure of D^{*0} and the strong decay $D^{*0} \to D^+\pi^-$.

I. INTRODUCTION

Three-body B decays have a much richer phenomenology with the number of decaying channels being about 10 times larger than the number in two-body decays. This provides another wonderful site to study the hadron spectroscopy and the intermediate resonant structures with the nontrivial kinematics described by two invariant masses of three-body final states. From the view of QCD, it is also important to investigate the nonresonant contribution in the factorization theorem [1]. In 2013, the LHCb Collaboration observed the appreciable local CP violation in the Dalitz plot of $B^\pm \to K^\pm\pi^+\pi^-$ and $B^\pm \to K^\pm K^+K^-$ decays [2], which switched on a new era to study the mater-antimatter asymmetry. In order to understand the physical observables in the full Dalitz plot with abundant phase space and complicated dynamics, the QCD-based approaches, such as the perturbative QCD (pQCD) approach [3–6] and QCD factorization (QCDF) approach [7–10], did some pioneering studies on the quasi-two-body B decays [11–24]. Furthermore, some

phenomenological analyses are also implemented within the U-spin, isospin, and flavor SU(3) symmetries for the relevant three-body B decays [25–30].

In the traditional framework of QCD-based approaches, $D^*_{(s)}$ is usually treated as a stable vector meson state by embodying the heavy quark effective theory (HQET) [31,32]. There are two categories for the single charm two-body B decays $B_{(s)} \to D^*_{(s)}h'$: one is the Cabibbo-Kobayashi-Maskawa (CKM) favored transition induced by the $b \to c$ decay [33,34], and the other one stems from the CKM suppressed $b \to u$ transition [35,36]. With the interplay between $b \to c$ and $b \to u$ transitions at tree level, the $B_{(s)} \to D^{(*)}_{(s)}K^{(*)}$ decays give the dominant constraint to the CKM angle γ [37]. Theoretical studies on this type of decay are carried out with the factorization-assisted topological-amplitude (FAT) approach [38], the QCDF approach [39], and also the pQCD approach [40–42]. Recently, collaborations at B factories [43–47] and LHC [48–52] have performed lots of Dalitz analysis of the processes $B_{(s)} \to D_{(s)}hh'$ and shown clearly the resonant structures $D^*_{(s)}$ in the $D_{(s)}h$ invariant mass spectroscopy, which without a doubt will enrich our knowledge of $D^*_{(s)}$ and promote us to study their contributions in the corresponding three-body B decays.

A new issue that has attracted attention recently in three-body B decays is the virtual contribution of a certain resonant state, whose pole mass is located lower than the

*physchai@hnu.edu.cn
†scheng@hnu.edu.cn
‡wfwang@sxu.edu.cn

invariant mass threshold of the final two mesons and the contribution that arose from the Breit-Wigner-tail (BWT) effect. Within the pQCD approach, the contribution from the BWT effect of $\rho(770)$ is found to be one half larger than the contribution from the pole mass of the first excited state $\rho(1450)$ in the channel $B^{\pm} \to \rho\pi^{\pm} \to K^+K^-\pi^{\pm}$ [53]. Inspired by the Belle [43], the *BABAR* [45], and the LHCb [49,52] Collaborations measurement of $B \to D\pi h$ decays, the BWT effects from the resonant state D^* are discussed in Ref. [54] and calculated in the pQCD approach with the invariant mass $m_{D\pi} > 2.1$ GeV [55], showing the indispensable role of $D^{*0}(2007)$ and $D^{*+}(2010)$ and indicating a ~5% contribution from the BWT effect to the branching ratios. In the channels with a resonant state D_s^*, some derivations from the single phase-space model have also been observed at B factories in the $B \to D_s K\pi(K)$ decays [46,47]. Moreover, the Dalitz plot analysis from the LHCb Collaboration indicates a rather large virtual contribution from D_s^{*-} in the $B_s^0 \to \bar{D}^0 K^- \pi^+$ decays [48]. These measurements motivate a systemic study of the BWT effect from $D_{(s)}^*$ in the three-body $B_{(s)} \to D_{(s)}hh'$ decays.

In this paper, we implement the pQCD approach to calculate the branching ratios of quasi-two-body decays $B_{(s)} \to D_{(s)}^*h' \to D_{(s)}hh'$ within a total of 46 channels, aiming to explore the role of different resonant states, especially to clarify the contributions from a possible BWT effect of the ground states D^* and D_s^*. We will not discuss the CP violation here since there is no contributions from penguin operators and hence, no CP asymmetry sources in the single charmed B decays. These types of quasi-two-body B decays happen in two phases, say, the weak decay of a b quark and the subsequent strong decay from the resonant states to two stable final states. The pQCD calculation is performed in the standard formalism of two-body B decays with replacing the single meson wave function by the dimeson one, in which the strong decays are represented by means of timelike form factor and parametrized by the relativistic Breit-Wigner function. We will also check the quasi-two-body decays in the narrow width approximation, with which the light cone distribution amplitude (LCDA) of a dimeson system shrinks into a delta function at the physical pole mass, and the result should directly recover the two-body calculation.

The rest of the paper is organized as follows. In Sec. II, we give a brief introduction for the theoretical framework. In Sec. III, the numerical results will be showed. Discussions and conclusions will be given in Sec. IV. Decaying amplitudes and the factorization formulas in the pQCD approach are collected in the Appendixes.

II. FRAMEWORK AND THE (DI)MESON WAVE FUNCTIONS

In the three-body hadronic B decays, all the events of the final states are restricted in the Daltz plot by considering four-momentum conservation. Different regions in the Dalitz plot correspond to special configurations of final particle momenta: (a) the three corners correspond to the configuration that one hadron is soft ($E_i \sim m_i$), and the other two are energetic and flying back-to-back [$E_{j,k} \sim (m_B - m_i)/2$]; (b) the intermediate parts of edges denote the kinematics that two hadrons move ahead with collinear momenta, and the rest one recoils back [$E_i \sim m_B/2$ and $E_j + E_k \sim m_B/2$ in the massless approximation of final mesons]; and (c) the central region in the Dalitz plot represents cases in which all three hadrons are energetic and move fast in the space in an approximately symmetric way ($E_{i,j,k} \sim m_B/3$). From the QCD side, the reliable perturbative calculation can only be carried out in the invariant mass region of (b) when the final mesons are all light due to the requirement of the factorization hypothesis (the energy scale to perform the perturbative calculation), so the physical problems in three-body hadronic B decays we can handle well so far as it is just for the resonant state dynamics, which is called quasi-two-body B decays. In the practice, the quasi-two-body B decays are usually treated as a marriage problem,[1] where the first ingredient is the weak decay described by the low energy effective Hamiltonian [56],

$$\mathcal{H}_{\text{eff}} = \frac{G_F}{\sqrt{2}} V_{qb}^* V_{q'd(s)}[C_1(\mu)O_1(\mu) + C_2(\mu)O_2(\mu)], \quad (1)$$

and the cascaded ingredient is the strong decay from the resonant state R to two stable mesons described by the matrix element $\langle M_1 M_2 | R \rangle$, with the energy eigenstate of R written by means of the Breit-Wigner formula or others. In the case of $B_{(s)} \to D_{(s)}^*h' \to D_{(s)}hh'$ as depicted in Fig. 1, $R = D_{(s)}^*$ and $q, q' \in \{c, u, d\}$; the decay amplitude can be intuitively understood by

$$\mathcal{A}(B_{(s)} \to Rh' \to D_{(s)}hh')$$

$$= \langle D_{(s)}h | R \rangle \frac{1}{[m_R^2 - s - im_R\Gamma_R(s)]} \langle Rh' | \mathcal{H}_{\text{eff}} | B_{(s)} \rangle, \quad (2)$$

where the two matrix elements demonstrating different interactions can be studied separately by different approaches, and many nonperturbative parameters are involved. In order to calculate the quasi-two-body decaying

---

[1]The factorization hypothesis is the basic idea of QCD-based approaches to deal with two-body B decays, where the hard scattering amplitude and nonperturbative LCDAs are convoluted in a general formula. Considering the weak decay at the quark level treated by the low energy effective theory and the nonperturbative LCDAs of single mesons, and the subsequent strong decay at the hadron level described by a timelike form factor, we mark that the quasi-two-body B decays are actually a type of marriage problem that involves both the perturbative calculation and the nonperturbative study of the dimeson LCDAs.
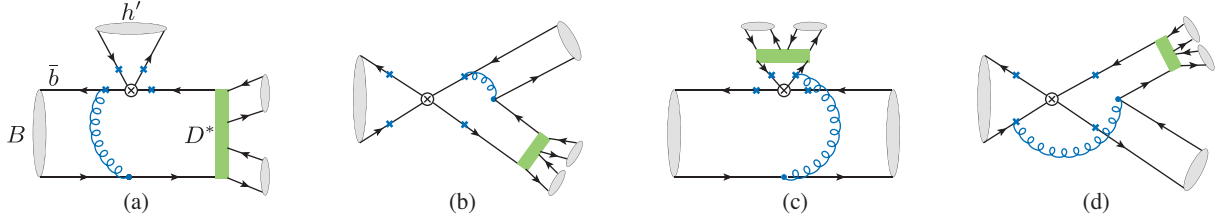
FIG. 1. Typical feynman diagrams for the decay processes $B_{(s)} \to D^*_{(s)} h' \to D_{(s)} h h'$, $h = (\pi, K)$, $h' = (\pi, K)$. The symbol $\otimes$ and $\times$ denote the weak vertex and all the possible attachments of hard gluons, respectively; the green rectangle represents the vector states $D^*_{(s)}$.

amplitudes in an unitive theoretical framework with reducing the number of nonperturbative parameters as much as possible, the dimeson wave function, supplementing to the single meson wave functions, is introduced in the pQCD approach to describe all the internal dynamics happened after the weak b decay. The decaying amplitudes are exactly written as a convolution of the hard kernel H with the hadron distribution amplitudes (DAs) ϕ_B, $\phi_{h'}$ and $\phi_{D_{(s)}h}$,

$$\mathcal{A}(B_{(s)} \to Rh' \to D_{(s)}hh') \equiv \langle [D_{(s)}h]_R h' | \mathcal{H}_{\text{eff}} | B_{(s)} \rangle$$
$$= \phi_B(x_1, b_1, \mu) \otimes H(x_i, b_i, \mu) \otimes \phi_{Dh}(x, b, \mu)$$
$$\otimes \phi_{h'}(x_3, b_3, \mu), \tag{3}$$

in which $[D_{(s)}h]_R$ indicates the dimeson system that we are interested in, μ is the factorization scale, and b_i are the conjugate distances of transversal momenta. We present the expressions of amplitudes $\mathcal{A}$ for the considered decaying processes in the Appendixes.

We use the conventional kinematics in the light cone coordinate under the rest frame of the B meson for the case of quasi-two-body charmed B decays,

$$p_1 = \frac{m_B}{\sqrt{2}}(1, 1, 0_T), \qquad k_1 = \left(0, x_1 \frac{m_B}{\sqrt{2}}, k_{1T}\right),$$
$$p_R = \frac{m_B}{\sqrt{2}}(1, \zeta, 0_T), \qquad k_R = \left(x_R \frac{m_B}{\sqrt{2}}, 0, k_{RT}\right),$$
$$p_3 = \frac{m_B}{\sqrt{2}}(0, 1-\zeta, 0_T), \qquad k_3 = \left(0, x_3(1-\zeta)\frac{m_B}{\sqrt{2}}, k_{3T}\right). \tag{4}$$

Here, p_1 and k_1 represent the momentum of B meson and the light spectator quark in B meson, respectively, with x_1 being the longitudinal momentum fraction. The momentum of the resonance $D^*_{(s)}$ and the pseudoscalar meson h' are denoted by p_R and p_3, with the longitudinal momentum fractions x_R and x_3, respectively. The variable $\zeta \equiv p_R^2/m_B^2 = s/m_B^2$ describes the momentum transfer from a B meson to a resonance R, which in general is a function of the invariant mass of the dimeson system decayed from the resonance, and $\sqrt{\zeta} = m_{D^*_{(s)}}/m_B$ when the invariant mass locates on the pole mass of the resonance $\sqrt{s} = m_{D^*_{(s)}}$.

Quasi-two-body charmed B decays are more complicated than the charmless decays since they involve three scales, the mass of a B meson (m_B), the invariant mass of a $D^*_{(s)}$ resonance ($|p_R| = \sqrt{s}$), and the mass difference of the heavy mesons and their corresponding heavy quarks ($\bar{\Lambda} \sim m_B - m_b \sim \sqrt{s} - m_c$), which is of the order of the QCD scale Λ_{QCD}. To construct a reasonable pQCD formulism of charmed B decays, the following hierarchies are postulated [32]:

$$m_B \gg \sqrt{s} \gg \bar{\Lambda}, \tag{5}$$

in which the first hierarchy guarantees the power counting analysis of the hard decaying amplitude at a large recoil, and the second hierarchy justifies the power expansion in the definition of light cone wave functions of resonant charm mesons (the dimeson system). In our calculation, we take into account only the leading twist wave functions of the heavy meson and dimeson system, say, B and $D_{(s)}h$, and take the light meson wave functions up to a twist three level with the chiral mass m_0^π and m_0^K, then only the powers $\mathcal{O}(m_c/m_B \equiv r_c)$ and $\mathcal{O}(m_0^\pi/m_B \equiv r_0)$, and the momentum transfer parameter ζ appear in the expressions of charmed two-body B decaying amplitudes. In this way, the reliability of pQCD approach can be checked at least at the leading power of $\mathcal{O}(r_c)$ for the charmed B decays [32–36], and in this paper, we are working at this accuracy.

We now move to the definitions of single and dimeson wave functions involved in the pQCD formulated Eq. (3). B meson DAs are defined under the HQET by the dynamical twist expansion [57]; at the leading twists level, the nonlocal matrix element associated with B meson for pQCD calculation is

$$\int d^4 z_1 e^{i\bar{k}_1 \cdot z_1} \langle 0 | \bar{d}_\sigma(z_1) b_\beta(0) | \bar{B}^0(p_1) \rangle$$
$$= \frac{-if_B}{4N_c} \left\{ (\not{p}_1 + m_B)\gamma_5 \left[\phi_B(x_1, b_1) - \frac{\not{n}_+ - \not{n}_-}{\sqrt{2}} \bar{\phi}_B(x_1, b_1) \right] \right\}_{\beta\sigma}, \tag{6}$$

where the antiquark momentum aligns on the minus direction on the light cone with the momentum fraction $x_1 = k_1^-/p_1^-$. The transversal projection term is omitted, and the integral $\varphi_\pm(x_1, b_1) = \int dk_1^+ d^2\mathbf{k}_{1\,\text{T}} e^{i\mathbf{k}_{1\,\text{T}} \cdot \mathbf{b}_1} \varphi_\pm(k_1)$

is underlined. The DA $\bar{\phi}_B$ is highly suppressed by $\mathcal{O}(\ln(\bar{\Lambda}/m_B))$ in contrast to ϕ_B [58]; we are working in the symmetry limit where $\bar{\phi}_B = 0$ to match with the current accuracy. The expression of DA is usually parametrized in the exponential model,

$$\phi_B(x_1, b_1) = N_B x_1^2 (1 - x_1)^2 \exp\left[-\frac{x_1^2 m_B^2}{2\omega_B^2} - \frac{(\omega_B b_1)^2}{2}\right], \quad (7)$$

with the normalization condition,

$$\int_0^1 dx_1 \phi_B(x_1, b_1 = 0) = 1; \quad (8)$$

the first inverse moment is taken as $\omega_B = 2/3\bar{\Lambda}$ [59,60].

The wave function of the single pseudoscalar meson $h' = \pi$, K is defined by the nonlocal matrix element [61,62]; we here take π^-, for example,

$$\int d^4 z_2 e^{ik_3 \cdot z_3} \langle \pi^-(p_3)|\bar{d}_\delta(z_3) u_\alpha(0)|0\rangle$$
$$= \frac{-if_\pi}{4N_c}\{\gamma_5[\not{p}_3 \phi_\pi(x_3, b_3) + m_0^\pi \phi_\pi^p(x_3, b_3) + m_0^\pi(\not{n}_- \not{n}_+ - 1)\phi_\pi^t(x_3, b_3)]\}_{\alpha\delta}. \quad (9)$$

Once again, the integral $\phi_\pi(x_3, b_3) = \int dk_3^+ d^2\mathbf{k}_{3\,\mathbf{T}} \times e^{i\mathbf{k}_{3\,\mathbf{T}} \cdot \mathbf{b}_3} \phi_\pi(k_3)$ is indicated. The decay constant f_π reflects the local matrix element between the vacuum and the pion meson state,

$$\langle \pi^+(p)|\bar{u}(0)(\mp \gamma_\tau \gamma_5)d(0)|0\rangle = \pm if_\pi p_\tau. \quad (10)$$

In the expression of Eq. (9), ϕ_π is the leading twist LCDA, and $\phi_\pi^{p(t)}$ are the twist three ones. The light cone vectors are defined as $n_+ = (1, 0, 0)$ and $n_- = (0, 1, 0)$, the chiral mass $m_0^\pi \equiv m_\pi^2/(m_u + m_d)$ originates from the equation of motion.

Because the transversal polarized vector meson does not contribute in $B \to VP$ decays, we only take into account the longitudinal polarized wave function of the $D_s h$ system. The hierarchy $m_B \gg \sqrt{s}$ makes sure that the wave function of the energetic $D_s h$ system absorbs the collinear dynamics but with the charm quark line being eikonalized. This is to say, the definition of charmed meson/dimeson system wave function is the mixing of the definitions of B meson wave function and the pion meson wave function, which are dominated by soft and collinear dynamics, respectively. The P-wave component of $D_{(s)}h$ system with a possible resonance $D_{(s)}^*$ is quoted as [31,32]

$$\Phi_{D_{(s)}h}^{\mathrm{P}} = \frac{1}{\sqrt{2N_c}} \not{\epsilon}_L (\not{p}_R + \sqrt{s}) \phi_{D_{(s)}h}(x, b, s). \quad (11)$$

At leading twist, the LCDA has the same Gegenbauer expansion as the vector meson $D_{(s)}^*$,

$$\phi_{D_{(s)}h}(x, b, s) = \frac{F_{D_{(s)}h}(s)}{2\sqrt{2N_c}} 6x(1 - x)[1 + a_{D_{(s)}h}(1 - 2x)]$$
$$\times \exp\left[-\frac{\omega_{D_{(s)}h}^2 b^2}{2}\right]. \quad (12)$$

In the P-wave $D_{(s)}h$ system, the total factor reflecting the normalization is presented by the more general timelike form factor $F_{D_{(s)}h}(s)$, which in the case of a single $D_{(s)}^*$ meson ($\sqrt{s} = m_{D_{(s)}^*}$) reduces to the decay constant $f_{D_{(s)}^*}$. In the $D_{(s)}^*$ dominant approximation, this form factor is defined and expressed as

$$F_{D_{(s)}h}(s) \equiv \frac{s\bar{p}_R^\mu \langle D_{(s)}h|\bar{c}\gamma_\mu(1 - \gamma_5)q|0\rangle}{[s^2 - 2s(m_{D_{(s)}}^2 + m_h^2) + (m_{D_{(s)}}^2 - m_h^2)^2]}$$
$$\to \frac{\sqrt{s} f_R g_{RD_{(s)}h}}{[m_R^2 - s - im_R\Gamma_R(s)]}, \quad (13)$$

where f_R is the decay constant of the resonant state, $\bar{p}_R$ denotes the momentum difference of $D_{(s)}$ and h mesons in the $D_{(s)}h$ system, and the strong coupling is defined by means of the matrix element $g_{RD_{(s)}h} \equiv \langle D_{(s)}h|R\rangle$. We present the derivation of this approximation expression in Appendix B. With the precise measurement of $g_{D^*D^0\pi^+} = 16.92 \pm 0.13 \pm 0.14$ [63,64] and the universal relation [65],

$$\frac{g_{D^*D\pi^\pm} f_\pi}{2\sqrt{m_{D^*}m_D}} = \frac{g_{D^*D_s K} f_K}{2\sqrt{m_{D^*}m_{D_s}}} = \frac{g_{D_s^*DK} f_K}{2\sqrt{m_{D_s^*}m_D}} = g, \quad (14)$$

we obtain $g_{D_s^*DK} = 14.6 \pm 0.06 \pm 0.07$ and $g_{D^*D_s K} = 14.6 \pm 0.10 \pm 0.13$. They are consistent with the result $g_{D_s^*DK} = 14.6 \pm 1.7$ and $g_{D^*D_s K} = 14.7 \pm 1.7$ [66] that are extracted from the CLEO Collaboration [67], and also comparable to the predictions $g_{D_s^*DK} = 15.2$, $g_{D^*D_s K} = 15.2$ obtained from the quark model [68]. By the way, a_{Dh} is the first Gegenbauer coefficient in the polynomial expansion, ω_{Dh} denotes the first inverse momentum of the P-wave $D_{(s)}h$ state, for these two parameters, and we use the values of their partner vector meson $D_{(s)}^*$ in the numerical evaluation.

For the sake of generality, we go beyond the narrow resonance approximation and take the energy dependent width [48–52],

$$\Gamma_R(s) = \Gamma_R^{\text{tot}}\left(\frac{\beta(s)}{\beta_R}\right)^3\left(\frac{s}{m_R^2}\right)X^2(qr_{\text{BW}}), \qquad (15)$$

in which Γ_R^{tot} is the total decay width of the resonant state. The nondimensional phase space factor $\beta(s)$ of $D_{(s)}h$ system is defined by

$$\beta(s) = \frac{1}{2s}\sqrt{[s-(m_{D_{(s)}}+m_h)^2][s-(m_{D_{(s)}}-m_h)^2]}, \quad (16)$$

and $\beta_R \equiv \beta(m_R)$. In our case of the P-wave configuration with $L=1$, the Blatt-Weisskopf barrier form factors $X(z)$ are [69]

$$X^2(qr_{\text{BW}}) = \left(\frac{1+m_R^2[\beta_R r_{\text{BW}}]^2}{1+s[\beta(s)r_{\text{BW}}]^2}\right), \qquad (17)$$

where the radius of the barrier is taken at $= 4.0$ GeV$^{-1} \sim$ 0.8 fm for all resonances [70]. To obtain the result in Eq. (17), we have implemented the relation $\beta(s) \equiv q/\sqrt{s}$ between the phase space factor and the magnitude of momentum for the daughter meson $D_{(s)}$ or h.

The total width of the charged vector D^* meson is precisely measured as $\Gamma_{D^{*+}}^{\text{tot}} = 83.4 \pm 1.8$ KeV, while the width of its strange partner meson D_s^* is only restricted by the upper limit $\Gamma_{D_s^{*+}}^{\text{tot}} = 1.9$ MeV so far [71]. There are some theoretical attempts to calculate the partial width of D_s^* meson; for example, the dominant partial width $\Gamma_{D_s^* \to D_s\gamma} = 0.066 \pm 0.026$ KeV is obtained in the radiative decay from lattice QCD evaluation [72], while the prediction from QCD sum rules is about 10 times larger ($\Gamma_{D_s^* \to D_s\gamma} = 0.59 \pm 0.15$ KeV) [73], and the second dominant partial width $\Gamma_{D_s^* \to D_s\pi^0} = 8.1_{-2.6}^{+3.0}$ eV is obtained from the heavy meson chiral perturbation [74]. We will use the upper limit value in the numerical evaluation to consider the largest uncertainty.[2] For the neutral vector D meson, the result from the isospin analysis $\Gamma_{D^{*0}}^{\text{tot}} = 55.3 \pm 1.4$ KeV [75] consists of the value (53 KeV) that we have extracted in the previous work [55]. In order to access the virtual contributions (BWT effect) from the state $D_{(s)}^*$ whose pole mass is lower than the threshold value of the invariant mass, i.e., $m_R < m_D + m_h$, the pole mass m_R in β_R shall be replaced by the effective mass m_0^{eff} to avoid the kinematical singularity that appeared in the phase space factor $\beta(s)$ [49],

---

[2]This value is also employed by the LHCb Collaboration in the study of the virtual contribution from D_s^* in the decaying channel $B_s^0 \to \bar{D}^0 K^- \pi^+$ [48].

$$m_0^{\text{eff}}(m_0) = m^{\text{min}} + (m^{\text{max}} - m^{\text{min}})$$
$$\times \left[1 + \tanh\left(\frac{m_0 - (m^{\text{max}}+m^{\text{min}})/2}{m^{\text{max}} - m^{\text{min}}}\right)\right], \qquad (18)$$

where $m_0^{\text{eff}} = m_{D_{(s)}} - m_{h'}$ and $m^{\text{min}} = m_{D_{(s)}} + m_h$ are the upper and lower thresholds of $\sqrt{s}$, respectively.

The differential branching ratios for the quasi-two-body $B_{(s)} \to D_{(s)}^* h' \to D_{(s)}hh'$ decays are written as

$$\frac{d\mathcal{B}}{d\zeta} = \frac{\tau_B q_{h'}^3 q^3}{48\pi^3 m_B^5}|\mathcal{A}|^2, \qquad (19)$$

in which $q_{h'}$ is the magnitude of momentum for the bachelor meson h',

$$q_{h'} = \frac{1}{2}\sqrt{[(m_B^2-m_{h'}^2)^2 - 2(m_B^2+m_{h'}^2)s + s^2]/s}. \quad (20)$$

III. NUMERICS AND DISCUSSIONS

In Table I, we list the masses, decay constants, and total widths of the mesons involved in the quasi-two-body decays. We take the masses and widths from PDG [71], use the decay constants updated from the Laplace QCD sum rules for the light and D^* mesons [76], and use the four-flavor lattice QCD result for the B mesons decay constants [77]. For the first inverse moments of heavy mesons, we take $\omega_{D^{*0}} = \omega_{D^{*\pm}} = 100 \pm 20$ MeV and $\omega_{D_s^{*0}} = 200 \pm 40$ MeV for the vector charmed mesons and take $\omega_{B^0} = \omega_{B^\pm} = 400 \pm 40$ MeV and $\omega_{B_s^0} = 500 \pm 50$ MeV for the B mesons [78]. The Gegenbauer moments in the leading twist LCDAs of light mesons are taken from the QCD sum rules [61] as $a_2^\pi = a_2^K = 0.25$, $a_1^K = 0.06$, and the moments of vector D meson are taken from the pQCD fitting with the $B \to D^*P$, D^*V decays data [41] as $a_1^{D^{*0}} = a_1^{D^{*\pm}} = 0.5 \pm 0.1$ and $a_1^{D_s^{*0}} = 0.4 \pm 0.1$. Besides these, the CKM matrix elements in the effective Hamiltonian are

TABLE I. Masses, decay constants, and total widths of the mesons involved in the quasi-two-body decays.

Meson	m(MeV)	f_M(MeV)	$\Gamma_{D^*}^{\text{tot}}$(KeV)/$\tau_B(10^{-12}$ s)
$\pi^\pm/\pi^0$	140/135	130 [76]	$\cdots$
$K^\pm/K^0$	494/498	156 [76]	$\cdots$
$D^{*\pm}$	2010	250 ± 11 [76]	83.4 ± 1.8
D^{*0}	2007	250 ± 11 [76]	55.3 ± 1.4 [75]
$D_s^{*\pm}$	2112	270 ± 19 [76]	< 1900
$B^\pm$	5279	189 [77]	1.638 ± 0.004
B^0	5280	189 [77]	1.520 ± 0.004
B_s^0	5367	231 [77]	1.509 ± 0.004

TABLE II. The pQCD predictions of the branching ratios for quasi-two-body decays $B^0 \to D^*_{(s)}h' \to Dhh'$, where the result of the channels happened by the BWT effect are denoted by $\mathcal{B}_v$. Theoretical uncertainties come from the inputs of ω_B, f_{D^*}, a_{Dh}, A, ω_{Dh} in turn.

Decay modes	$\mathcal{B}/\mathcal{B}_v$	Results	Units
$B^0 \to D^{*-}\pi^+ \to \bar{D}^0\pi^-\pi^+$	$\mathcal{B}$	$1.69^{+0.57+0.15+0.13+0.07+0.04}_{-0.52-0.15-0.11-0.05-0.02}$	10^{-3}
$\to D^-\pi^0\pi^+$	$\mathcal{B}$	$7.79^{+3.70+0.70+0.58+0.33+0.25}_{-2.34-0.67-0.69-0.23-0.13}$	10^{-4}
$\to D_s^-K^0\pi^+$	$\mathcal{B}_v$	$1.25^{+0.62+0.11+0.10+0.05+0.02}_{-0.38-0.11-0.09-0.04-0.04}$	10^{-5}
$B^0 \to D^{*+}\pi^- \to D^0\pi^+\pi^-$	$\mathcal{B}$	$1.01^{+0.39+0.09+0.00+0.04+0.02}_{-0.25-0.08-0.00-0.03-0.01}$	10^{-6}
$\to D^+\pi^0\pi^-$	$\mathcal{B}$	$4.64^{+1.72+0.41+0.03+0.18+0.01}_{-1.22-0.40-0.00-0.13-0.02}$	10^{-7}
$\to D_s^+\bar{K}^0\pi^-$	$\mathcal{B}_v$	$1.64^{+0.59+0.15+0.00+0.06+0.00}_{-0.42-0.14-0.00-0.04-0.00}$	10^{-8}
$B^0 \to D^{*-}K^+ \to \bar{D}^0\pi^-K^+$	$\mathcal{B}$	$1.38^{+0.64+0.16+0.04+0.06+0.04}_{-0.42-0.09-0.10-0.04-0.03}$	10^{-4}
$\to D^-\pi^0K^+$	$\mathcal{B}$	$6.39^{+2.78+0.57+0.56+0.27+0.05}_{-2.13-0.56-0.52-0.19-0.28}$	10^{-5}
$\to D_s^-K^0K^+$	$\mathcal{B}_v$	$1.02^{+0.48+0.10+0.09+0.04+0.03}_{-0.31-0.09-0.08-0.03-0.02}$	10^{-6}
$B^0 \to \bar{D}^{*0}\pi^0 \to \bar{D}^0\pi^0\pi^0$	$\mathcal{B}$	$1.05^{+0.45+0.10+0.02+0.05+0.03}_{-0.27-0.09-0.00-0.03-0.02}$	10^{-4}
$\to D^-\pi^+\pi^0$	$\mathcal{B}_v$	$1.02^{+0.37+0.10+0.02+0.04+0.01}_{-0.27-0.09-0.02-0.03-0.01}$	10^{-5}
$\to D_s^-K^+\pi^0$	$\mathcal{B}_v$	$2.39^{+0.94+0.23+0.00+0.11+0.02}_{-0.66-0.22-0.02-0.07-0.03}$	10^{-6}
$B^0 \to D^{*0}K^0 \to D^0\pi^0K^0$	$\mathcal{B}$	$9.49^{+2.57+0.85+0.40+0.38+0.19}_{-1.76-0.81-0.46-0.27-0.14}$	10^{-7}
$\to D^+\pi^-K^0$	$\mathcal{B}_v$	$6.32^{+2.50+0.58+0.15+0.26+0.02}_{-1.69-0.54-0.15-0.17-0.05}$	10^{-8}
$\to D_s^+K^-K^0$	$\mathcal{B}_v$	$9.89^{+2.65+0.90+0.42+0.40+0.21}_{-2.05-0.90-0.47-0.28-0.15}$	10^{-9}
$B^0 \to \bar{D}^{*0}K^0 \to \bar{D}^0\pi^0K^0$	$\mathcal{B}$	$1.66^{+0.88+0.15+0.04+0.07+0.01}_{-0.45-0.14-0.05-0.03-0.02}$	10^{-5}
$\to D^-\pi^+K^0$	$\mathcal{B}_v$	$1.55^{+0.62+0.14+0.00+0.07+0.03}_{-0.43-0.13-0.00-0.05-0.03}$	10^{-6}
$\to D_s^-K^+K^0$	$\mathcal{B}_v$	$3.46^{+1.36+0.31+0.00+0.15+0.03}_{-0.94-0.30-0.00-0.10-0.03}$	10^{-7}

determined by the Wolfenstein parameters $\lambda = 0.22650 \pm 0.00048$, $A = 0.790^{+0.017}_{-0.012}$, $\bar{\rho} = 0.141^{+0.016}_{-0.017}$, and $\bar{\eta} = 0.357 \pm 0.01$ [71]; the masses of D mesons are also taken from PDG with $m_{D^0} = 1.865$ GeV, $m_{D^\pm} = 1.870$ GeV, and $m_{D_s^\pm} = 1.968$ GeV; and the chiral masses of light mesons are chosen at $m_0^\pi = 1.4 \pm 0.1$ GeV and $m_0^K = 1.9 \pm 0.1$ GeV [78],

Our predictions for a total of 46 channels of quasi-two-body decays $B^0/B^+/B_s^0 \to D^*_{(s)}h' \to D_{(s)}hh'$ are collected in Tables II–IV in turn. In each table, all the possible P-wave resonances $D^*_{(s)}$ are presented to clarify the strength of the weak interactions in two-body $B_{(s)}$ decays, and the power hierarchy for the result of different two-body decays $B_{(s)} \to D^*_{(s)}h'$ can be read from the weak decay amplitudes presented in Appendix A. For example, the channel $B^0 \to D^{*-}\pi^+$ is first color allowed, and second, both the emission and annihilation typological diagrams give contributions. The channel $B^0 \to D^{*-}K^+$ is CKM suppressed $[\mathcal{O}(\lambda)]$ with

TABLE III. The same as Table II, but for the quasi-two-body $B^+ \to D^*_{(s)}h' \to Dhh'$ decaying channels.

Decay modes	$\mathcal{B}/\mathcal{B}_v$	Results	Units
$B^+ \to D^{*+}\pi^0 \to D^0\pi^+\pi^0$	$\mathcal{B}$	$5.81^{+1.45+0.52+0.03+0.23+0.05}_{-1.20-0.50-0.05-0.16-0.02}$	10^{-7}
$\to D^+\pi^0\pi^0$	$\mathcal{B}$	$2.65^{+0.70+0.24+0.00+0.10+0.01}_{-0.46-0.23-0.03-0.07-0.00}$	10^{-7}
$\to D_s^+\bar{K}^0\pi^0$	$\mathcal{B}_v$	$9.04^{+3.04+0.89+0.03+0.36+0.01}_{-2.26-0.79-0.01-0.25-0.01}$	10^{-9}
$B^+ \to \bar{D}^{*0}\pi^+ \to \bar{D}^0\pi^0\pi^+$	$\mathcal{B}$	$3.22^{+1.30+0.29+0.09+0.13+0.05}_{-0.94-0.28-0.22-0.09-0.03}$	10^{-3}
$\to D^-\pi^+\pi^+$	$\mathcal{B}_v$	$2.33^{+0.98+0.21+0.13+0.10+0.04}_{-0.72-0.20-0.16-0.07-0.05}$	10^{-4}
$\to D_s^-K^+\pi^+$	$\mathcal{B}_v$	$3.52^{+1.54+0.32+0.17+0.15+0.06}_{-1.03-0.30-0.17-0.10-0.07}$	10^{-5}
$B^+ \to \bar{D}^{*0}K^+ \to \bar{D}^0\pi^0K^+$	$\mathcal{B}$	$2.46^{+1.18+0.14+0.16+0.10+0.09}_{-0.69-0.28-0.10-0.07-0.01}$	10^{-4}
$\to D^-\pi^+K^+$	$\mathcal{B}_v$	$1.80^{+0.84+0.16+0.11+0.07+0.03}_{-0.54-0.15-0.10-0.05-0.04}$	10^{-5}
$\to D_s^-K^+K^+$	$\mathcal{B}_v$	$2.63^{+1.18+0.24+0.13+0.11+0.04}_{-0.79-0.23-0.13-0.08-0.05}$	10^{-6}
$B^+ \to D^{*0}K^+ \to D^0\pi^0K^+$	$\mathcal{B}$	$1.00^{+0.28+0.05+0.01+0.04+0.02}_{-0.30-0.11-0.02-0.03-0.01}$	10^{-6}
$\to D^+\pi^-K^+$	$\mathcal{B}_v$	$5.92^{+2.23+0.53+0.12+0.24+0.05}_{-1.53-0.51-0.08-0.16-0.04}$	10^{-8}
$\to D_s^+K^-K^+$	$\mathcal{B}_v$	$1.10^{+0.42+0.12+0.01+0.04+0.00}_{-0.31-0.11-0.02-0.03-0.00}$	10^{-8}

TABLE IV.   The same as Table II, but for the quasi-two-body $B^0_s \to D^*_{(s)} h' \to Dhh'$ decaying channels.

Decay modes	$\mathcal{B}/\mathcal{B}_v$	Results	Units
$B^0_s \to D^{*-}_s \pi^+ \to \bar{D}^0 K^- \pi^+$	$\mathcal{B}_v$	$1.90^{+0.94+0.28+0.16+0.08+0.14}_{-0.59-0.26-0.14-0.06-0.15}$	10^{-5}
$\to D^- \bar{K}^0 \pi^+$	$\mathcal{B}_v$	$1.83^{+0.94+0.27+0.15+0.08+0.14}_{-0.57-0.25-0.13-0.06-0.14}$	10^{-5}
	$\cdots$	$\cdots$	$\cdots$
$B^0_s \to D^{*-}_s K^+ \to \bar{D}^0 K^- K^+$	$\mathcal{B}_v$	$1.28^{+0.66+0.19+0.10+0.06+0.10}_{-0.42-0.17-0.09-0.04-0.10}$	10^{-6}
$\to D^- \bar{K}^0 K^+$	$\mathcal{B}_v$	$1.23^{+0.66+0.18+0.09+0.05+0.09}_{-0.40-0.17-0.09-0.04-0.10}$	10^{-6}
	$\cdots$	$\cdots$	$\cdots$
$B^0_s \to D^{*-} \pi^+ \to \bar{D}^0 \pi^- \pi^+$	$\mathcal{B}$	$8.61^{+0.76+0.77+0.84+0.37+0.19}_{-0.84-0.74-0.97-0.26-0.21}$	10^{-7}
$\to D^- \pi^0 \pi^+$	$\mathcal{B}$	$3.82^{+0.70+0.34+0.36+0.16+0.06}_{-0.23-0.33-0.29-0.12-0.08}$	10^{-7}
$\to D^-_s K^0 \pi^+$	$\mathcal{B}_v$	$5.50^{+0.44+0.49+0.82+0.24+0.13}_{-0.48-0.47-0.73-0.17-0.13}$	10^{-9}
$B^0_s \to D^{*+} K^- \to D^0 \pi^+ K^-$	$\mathcal{B}$	$1.13^{+0.46+0.10+0.00+0.04+0.00}_{-0.31-0.10-0.00-0.03-0.00}$	10^{-6}
$\to D^+ \pi^0 K^-$	$\mathcal{B}$	$5.14^{+2.10+0.46+0.01+0.20+0.00}_{-1.41-0.44-0.00-0.14-0.00}$	10^{-7}
$\to D^+_s \bar{K}^0 K^-$	$\mathcal{B}_v$	$1.67^{+0.68+0.15+0.00+0.06+0.00}_{-0.46-0.14-0.00-0.04-0.00}$	10^{-8}
$B^0_s \to \bar{D}^{*0} \pi^0 \to \bar{D}^0 \pi^0 \pi^0$	$\mathcal{B}$	$4.16^{+0.24+0.37+0.50+0.18+0.07}_{-0.44-0.36-0.41-0.13-0.16}$	10^{-7}
$\to D^- \pi^+ \pi^0$	$\mathcal{B}_v$	$2.36^{+0.25+0.21+0.28+0.10+0.05}_{-0.21-0.20-0.27-0.07-0.06}$	10^{-8}
$\to D^-_s K^+ \pi^0$	$\mathcal{B}_v$	$2.75^{+0.23+0.25+0.41+0.12+0.06}_{-0.24-0.24-0.37-0.08-0.01}$	10^{-9}
$B^0_s \to \bar{D}^{*0} \bar{K}^0 \to \bar{D}^0 \pi^0 \bar{K}^0$	$\mathcal{B}$	$1.71^{+0.73+0.15+0.04+0.07+0.02}_{-0.56-0.15-0.04-0.05-0.08}$	10^{-4}
$\to D^- \pi^+ \bar{K}^0$	$\mathcal{B}_v$	$1.59^{+0.75+0.14+0.01+0.07+0.01}_{-0.50-0.14-0.00-0.05-0.02}$	10^{-5}
$\to D^-_s K^+ \bar{K}^0$	$\mathcal{B}_v$	$3.82^{+1.79+0.34+0.01+0.16+0.03}_{-1.18-0.33-0.00-0.12-0.04}$	10^{-6}

only the emission typology contributing to the amplitude, while the channel $B^0 \to D^{*+} \pi^-$ is CKM double suppressed $[\mathcal{O}(\lambda^2)]$ and simultaneously, color suppressed, which results in the branching ratios being 2 and 3 powers smaller in magnitude than those of the channel $B^0 \to D^{*-} \pi^+$, respectively. For each case of the two-body decay, we go a step further to show the possible different strong couplings between $D^*_{(s)}$ and the $D_{(s)} h$ state, say, with $\bar{u}u$, $\bar{d}d$ and $\bar{s}s$ configurations. Once again, we take the weak decay in channel $B^0 \to D^{*-} \pi^+$ as the example to explain more. The result of the strong decays in two channels with the u- and d-quark pair configurations obeys the isospin relation $g_{D^{*-} \bar{D}^0 \pi^-} = -\sqrt{2} g_{\bar{D}^{*-} D^- \pi^0}$; of course, this relation also works for other similar two channels, like $D^{*-} \to \bar{D}^0 \pi^-$ and $D^{*-} \to D^- \pi^0$, which are both happened by the pole mass dynamics ($m_{D^{*-}} > m_{\bar{D}^0} + m_{\pi^-}$, $m_{D^-} + m_{\pi^0}$). The strong decay $D^{*-} \to D^-_s K^0$ happens by the BWT effect, and the branching ratio is apparently much smaller with a comparison to the strong decays that happen by the pole mass dynamics.

In this work, we do not take into account the pure annihilation quasi-two-body decays, which is doubly suppressed by the CKM and color, because the pole mass contributions to their branching ratios are already rather small ($[10^{-12}, 10^{-8}]$), if we consider the branching ratio ($[10^{-2}, 10^{-1}]$) of the weak decay $D \to \pi K$ used to rebuild D mesons events. As shown in the Tables II–IV, the largest error in our prediction comes from the first inverse momentum of the $B_{(s)}$ meson ($\omega_{B_{(s)}}$), the second one comes from the decay constant of intermediate resonant

states ($f_{D^*_{(s)}}$), the Gegenbauer moment of resonant state (a_{Dh}) gives the third error, the Wolfenstein parameter (A) is the fourth uncertainty source, and the last uncertainty source is the inverse moment of resonant state (ω_{Dh}). For the decay channels $B^+ \to D^- \pi^+ \pi^+ (K^+)$ that happened by the BWT effect, the result in this work is a litter bit larger than the previous predictions [55]. The reason is that here we take the starting point of $D\pi$ invariant mass at their threshold value 2.01 GeV, while the evaluation is chosen to start at 2.1 GeV in the former work.

In Fig. 2, we depict the differential branching ratios of channels $B^0 \to D^{*-} \pi^+ \to Dh\pi^+$ and $B^+ \to \bar{D}^{*0} \pi^+ \to Dh\pi^+$ to reveal the relative strength in different strong couplings following a same two-body weak decay. The processes $D^{*-} \to \bar{D}^0 \pi^-$ (in red), $D^- \pi^0$ (in blue) happened by pole mass dynamics, and the process $D^{*-} \to D^-_s K^0$ (in magenta) happened by the BWT effect, following the same $B^0 \to \bar{D}^{*-} \pi^+$ weak decay, are shown explicitly on the left panel. In parallel, the pole mass dynamical process $\bar{D}^{*0} \to \bar{D}^0 \pi^0$ (in red) and the BWT induced processes $\bar{D}^{*0} \to D^- \pi^+$ (in blue), $D^-_s K^+$ (in magenta) following the $B^+ \to \bar{D}^{*0} \pi^+$ weak decay are shown on the right panel. Within the embedded graphs, we display the evolution of isospin ratios on the invariant mass,

$$R_{D^{*-} \to D\pi} \equiv \frac{d\mathcal{B}(B^0 \to D^{*-} \pi^+ \to D^- \pi^0 \pi^+)}{d\mathcal{B}(B^0 \to D^{*-} \pi^+ \to \bar{D}^0 \pi^- \pi^+)},$$

$$R_{\bar{D}^{*0} \to D\pi} \equiv \frac{d\mathcal{B}(B^+ \to \bar{D}^{*0} \pi^+ \to \bar{D}^0 \pi^0 \pi^+)}{d\mathcal{B}(B^+ \to \bar{D}^{*0} \pi^+ \to D^- \pi^+ \pi^+)}. \quad (21)$$
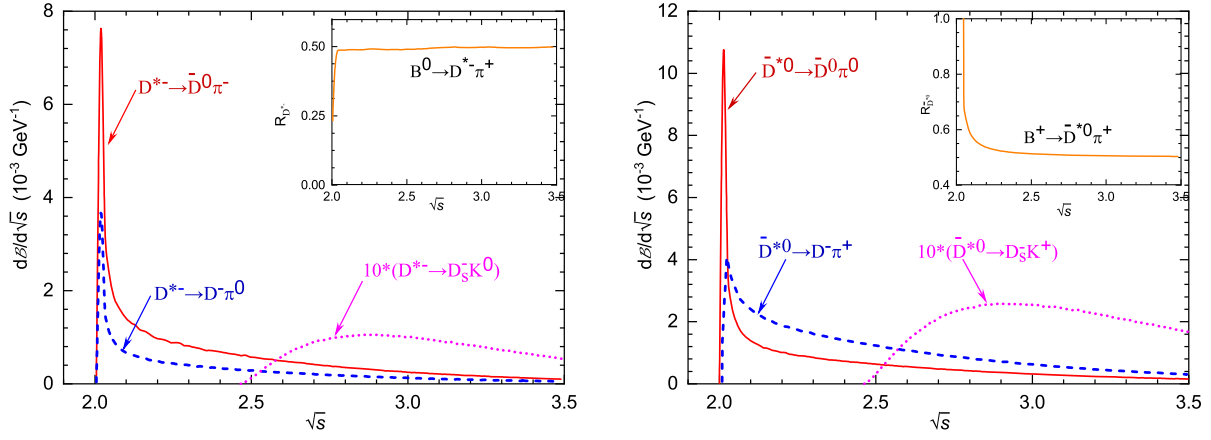
FIG. 2.   The differential branching ratios for the quasi-two-body $B^0 \to D^{*-}\pi^+ \to Dh\pi^+$ decays (left panel) and $B^+ \to \bar{D}^{*0}\pi^+ \to Dh\pi^+$ decays (right panel). The embedded graphs denote the ratios $R_{D^* \to D\pi}$.

It can be seem that the ratio $R_{D^{*\pm}}$ goes to 0.5 suddenly around the $D^{*\pm}$ pole, which is natural due to the pole mass dynamics for both the strong decays $D^{*-} \to D^-\pi^0$ and $D^{*-} \to \bar{D}^0\pi^-$. Nevertheless, the ratio $R_{D^{*0}}$ trends to 0.5 from infinity smoothly; the underlying reason is that the $\bar{D}^{*0} \to D^-\pi^+$ process happens by the BWT effect with the threshold value of $D^-\pi^+$ state being a little bit larger than the $\bar{D}^{*0}$ pole mass. Hence, the peak of its $d\mathcal{B}/d\sqrt{s}$ curve emerges at the invariant mass a little bit larger than the pole mass. Concerning the BWT effect in the channels $B^0 \to D^{*-}\pi^+ \to D_s^-K^0\pi^+$ and $B^+ \to D^{*0}\pi^+ \to D_s^-K^+\pi^+$ (in magenta) induced by the s-quark pair configuration, we multiply their result by 10 to show clearly the evolution behavior. Their curves are smooth, and the locations of the largest distribution (2.8–2.9 GeV) are far away from the resonance pole masses by 0.8–0.9 GeV with the threshold values of D_sK states being larger than their resonance pole masses by 0.455 GeV.

We plot the differential branching ratio of $B_s^0 \to D_s^{*-}\pi^+ \to \bar{D}^0K^-\pi^+$ decay with the invariant mass of $\bar{D}^0K^-$ state varying in [2.3, 4.0] GeV in Fig. 3; we also embed the evolution of total branching ratio on m_0.

(i)   As it is shown in the embedded graph, the total branching ratio does not displace a dependence on the effective mass; that is to say, the width effect in Eq. (15) of D_s^{*-} is negligible here. This can be understood by the Breit-Wigner expression in Eq. (2), where the real part is much larger than the imaginary part in the denominator, say, $|m_{D_s^{*-}}^2 - s| \gg |m_{D_s^{*-}}\Gamma_{D_s^{*-}}(s)|$, when $\sqrt{s} > 2.359$ GeV and the total width $\Gamma_{D_s^{*-}} < 1.9$ MeV.

(ii)   One can see that the BWT effect in this channel is at the same order as in the channels of $B^0 \to D^{*-}\pi^+ \to D_s^-K^0\pi^+$ and $B^+ \to \bar{D}^{*0}\pi^+ \to D_s^-K^+\pi^+$ (magenta curves in Fig. 2), even though the total decay width of D_s^* is about 20 larger than the width of D^*. This is not a surprise because the BWT effect is not sensitive

to the width but to the real part of the Breit-Wigner propagators, as we have demonstrated above.

(iii)   For the real part of the Breit-Wigner propagators in this channel, the threshold value 2.359 GeV is closer to the resonance pole mass $m_{D_s^{*-}} = 2.112$ GeV, compared to the interval between the dimeson threshold and resonance pole mass in the two B meson decaying channels (0.455 GeV), so the location of the largest distribution in this channel is closer to the $\bar{D}^0K^-$ threshold.

(iv)   We highlight that the BWT effect discussed in this work is not equal to the width effect of the intermediate resonances; it is determined by the real part of Breit-Wigner propagator since $|m_R^2 - s| \gg m_R\Gamma_R(s)$ in the case of $R = D_{(s)}^*$. That is why we get the significant contribution from the BWT effect for
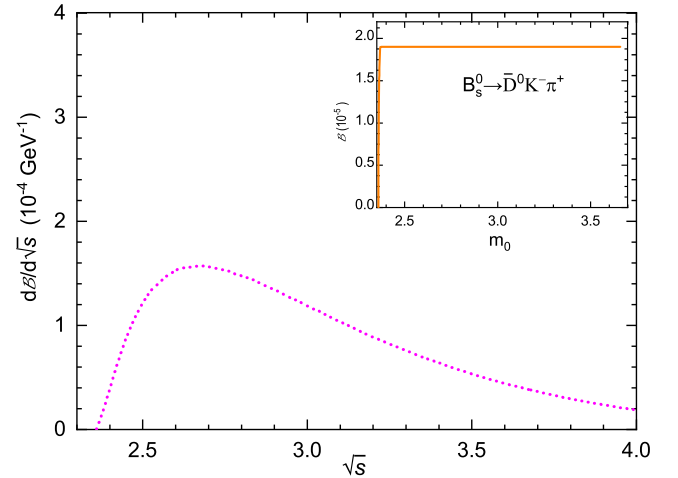

FIG. 3.   The differential branching ratios for the quasi-two-body decay $B_s^0 \to D_s^{*-}\pi^+ \to \bar{D}^0K^-\pi^+$ with the invariant mass $\sqrt{s} \in [2.3, 4.0]$ GeV. The embedded graph indicates the evolution on m_0 from the $\bar{D}^0K^-$ threshold value to m_0^{eff}.

TABLE V. The comparison between pQCD predictions and available experimental measurements for some channels happened by the BWT effect.

Decay modes	$\mathcal{B}_v(10^{-5})$	$\mathcal{B}_v^{\text{cut}}(10^{-5})$ [55]	Data (10^{-5})
$B^+ \to \bar{D}^{*0}\pi^+ \to D^-\pi^+\pi^+$	$23.3^{+10.1}_{-7.70}$	$19.2^{+8.80}_{-6.20}$	22.3 ± 3.20 [43]
			10.9 [45]
			10.9 ± 2.70 [52]
$B^+ \to \bar{D}^{*0}K^+ \to D^-\pi^+K^+$	$1.80^{+0.86}_{-0.57}$	$1.48^{+0.68}_{-0.47}$	0.56 ± 0.23 [49]
$B_s^0 \to D_s^{*-}\pi^+ \to \bar{D}^0K^-\pi^+$	$1.90^{+1.01}_{-0.68}$		4.70 ± 4.38 [48]

the quasi-two-body $B_{(s)} \to D_{(s)}^* h' \to D_{(s)}hh'$ decays, even though the total widths of $D_{(s)}^*$ mesons are rather small.

We compare our predictions with the available measurements for some channels induced by the BWT effect in Table V, where the theoretical and experimental errors are both added in quadrature. The result listed in the second column is obtained with the integral of invariant mass starting from the threshold value. Because the data of the first two channels are obtained by taking the integral with a cut $\sqrt{s} \geq 2.1$ GeV, which is a little bit larger than the threshold, we show that the pQCD predictions with the same cut in the third column, denoted by $\mathcal{B}_v^{\text{cut}}$. For the channel $B^+ \to \bar{D}^{*0}\pi^+ \to D^-\pi^+\pi^+$, the prediction is more inclined to the Belle data, but still with a large uncertainty. For the channel $B^+ \to \bar{D}^{*0}K^+ \to D^-\pi^+K^+$, the central value of pQCD prediction is about 2 times larger in magnitude than the LHCb measurement, even though a large uncertainty is associated with the experimental data. With consideration of the consistency between the measurements and the pQCD predictions for the relevant two-body weak decays $B^+ \to \bar{D}^{*0}\pi^+$ and $B^+ \to \bar{D}^{*0}K^+$ as shown in Table VI, we believe the result of these two channels $B^+ \to \bar{D}^{*0}\pi^+ \to D^-\pi^+\pi^-$ and $B^+ \to \bar{D}^{*0}K^+ \to D^-\pi^+K^+$ have a similar power behavior as displayed in Table V because they process the same strong decay. We hope that the Belle-II and the LHCb

Collaborations restudy these two channels to reveal the important information of D^{*0} and the strong decay $D^{*0} \to D^+\pi^-$. For the channel $B_s^0 \to D_s^{*-}\pi^+ \to \bar{D}^0K^-\pi^+$, the pQCD prediction is in the same power as the data; more data will explain more.

With the calculations for these quasi-two-body decays, we can extract the branching ratios of single charmed two-body B decays by using the narrow width approximation,

$$\mathcal{B}(B \to D_{(s)}^* h' \to D_{(s)}hh')$$
$$\approx \mathcal{B}(B \to D_{(s)}^* h') \cdot \mathcal{B}(D_{(s)}^* \to D_{(s)}h), \quad (22)$$

with the measurements $\mathcal{B}(D^{*+} \to D^0\pi^+) = 67.7\%$, $\mathcal{B}(D^{*+} \to D^+\pi^0) = 30.7\%$ and $\mathcal{B}(D^{*0} \to D^0\pi^0) = 64.7\%$ [71]. The result of the CKM favored channels is shown in Table VI, which is consistent with the direct two-body calculations and agree with the data. For the CKM suppressed decays, only the channel $B^+ \to D^{*0}K^+$ has been measured with the branching ratio $\mathcal{B}(B^+ \to D^{*0}K^+) = (7.8 \pm 2.2) \times 10^{-6}$ [71]; our extraction here gives $(1.54^{+0.45}_{-0.49}) \times 10^{-6}$, consisting of the result $(0.71^{+0.76}_{-0.53}) \times 10^{-6}$ by the direct two-body calculation from the pQCD approach [42], however, deviating from the data by 3σ. The result from FAT approach $(11.8^{+3.5}_{-3.5}) \times 10^{-6}$ is in agreement with the data because their nonfactorizable annihilation-type contribution is fit from data and much

TABLE VI. Branching ratios of $B_{(s)} \to D^*h'$ decays obtained from quasi-two-body processes under the narrow width approximation. The previous two-body pQCD calculation [41] and the experimental measurements are also listed for comparison.

Decay modes	pQCD (10^{-4})	This work (10^{-4})	Data (10^{-4}) [71]
$B^0 \to D^{*-}\pi^+$	$26.1^{+8.90}_{-9.50}$	$25.0^{+8.90}_{-8.10}$	27.4 ± 1.30
		$25.4^{+12.4}_{-8.20}$	
$B^0 \to D^{*-}K^+$	$2.21^{+0.82}_{-0.83}$	$2.04^{+0.98}_{-0.65}$	2.12 ± 0.15
		$2.08^{+0.94}_{-0.74}$	
$B^0 \to \bar{D}^{*0}\pi^0$	$2.30^{+0.87}_{-0.83}$	$1.62^{+0.71}_{-0.44}$	2.20 ± 0.60
$B^0 \to \bar{D}^{*0}K^0$	$0.25^{+0.10}_{-0.09}$	$0.26^{+0.14}_{-0.07}$	0.36 ± 0.12
$B^+ \to \bar{D}^{*0}\pi^+$	$51.1^{+14.7}_{-14.2}$	$49.8^{+20.7}_{-15.6}$	49.0 ± 1.70
$B^+ \to \bar{D}^{*0}K^+$	$3.94^{+1.24}_{-1.32}$	$3.80^{+1.86}_{-1.16}$	$3.97^{+0.31}_{-0.28}$
$B_s^0 \to \bar{D}^{*0}\bar{K}^0$	$4.14^{+2.01}_{-1.52}$	$2.64^{+1.15}_{-0.90}$	2.80 ± 1.10

larger than it was calculated with the pQCD approach. LHCb will accumulate much more data to clarify this problem.

IV. CONCLUSION

In this paper, we studied systematically the role of $D^*_{(s)}$ and their contributions in $B_{(s)} \to D_{(s)}hh'$ ($h' = \pi, K$) decays by taking the dimeson LCDAs of $D_{(s)}h$ system in the framework of the pQCD approach. With the weak decays $B_{(s)} \to D^*_{(s)}h'$ stemming only from the tree level current-current operator, there are no sources of weak phase differences to generate CP violations, so we predicted only the branching ratios. In the local kinematic region where the invariant mass of final $D_{(s)}h$ system locates in/around the interval of $D^*_{(s)}$ and simultaneously, the other invariant mass approaching zero, the three-body decay can be treated as a quasi-two-body decaying process and divided into two ingredients. The first one is the b quark weak decays which have the same formula as in the two-body B decays, and the strong decays that happened subsequently are absorbed into the dimeson wave functions of $D_{(s)}h$ system by means of the timelike form factor.

We calculated in total 46 channels for possible intermediate $D^*_{(s)}$ contributions in B^0, B^+, and B^0_s decays, and clarified the strong decays $D^*_{(s)} \to D_{(s)}h$ by u-, d-, and s-quark pair configurations for each resonant structure. Concerning the charged resonance $D^{*\pm}$, the strong decays with the u- and d-quark configurations happen by the pole mass dynamics, while the decay with s-quark configuration happens by the BWT effect. For the neutral resonances $\bar{D}^{*0}$

and D^{*0}, the strong decays with the u-quark configuration happen by the pole mass dynamics, and the d- and s-quark configurations happen by the BWT effect. The strong decays of D^*_s following from the B_s weak decay happen only by the BWT effect with both the u- and d-quark configurations. Our predictions certify the smallness ($< 5\%$) of the BWT effect in the three-body $B_{(s)}$ decays with the intermediate resonant states D^*, and the little tension between our predictions and the current data of the channels $B^+ \to \bar{D}^{*0}\pi^+(K^+) \to D^-\pi^+\pi^+(K^+)$ requires future measurements with high accuracy. For the quasi-two-body decay in the channel $B^0_s \to D^{*-}_s\pi^+ \to \bar{D}^0K^-\pi^+$ happened by the BWT effect, the pQCD prediction is consistent with the current LHCb measurement within a large error. We also checked the narrow width approximation of these resonant states by extracting the branching ratios of relative two-body decays from these quasi-two-body processes and found it works well for the CKM-favored channels.

ACKNOWLEDGMENTS

APPENDIX A: DECAY AMPLITUDES

The amplitudes of two-body decays $B_{(s)} \to D^*_{(s)}\pi$, $D^*_{(s)}K$ in the factorization approaches are [41,42]

$$\mathcal{A}(B^0 \to D^{*-}\pi^+) = \frac{G_F}{\sqrt{2}} V^*_{cb}V_{ud}\left[\left(\frac{c_1}{3} + c_2\right)F_{TD^*} + c_1 M_{TD^*} + \left(c_1 + \frac{c_2}{3}\right)F_{A\pi} + c_2 M_{A\pi}\right], \tag{A1}$$

$$\mathcal{A}(B^0 \to D^{*+}\pi^-) = \frac{G_F}{\sqrt{2}} V^*_{ub}V_{cd}\left[\left(c_1 + \frac{c_2}{3}\right)F_{AD^*} + c_2 M_{AD^*} + \left(\frac{c_1}{3} + c_2\right)F_{T\pi} + c_1 M_{T\pi}\right], \tag{A2}$$

$$\mathcal{A}(B^0 \to D^{*-}K^+) = \frac{G_F}{\sqrt{2}} V^*_{cb}V_{us}\left[\left(\frac{c_1}{3} + c_2\right)F_{TD^*} + c_1 M_{TD^*}\right], \tag{A3}$$

$$\mathcal{A}(B^0 \to \bar{D}^{*0}\pi^0) = \frac{G_F}{2} V^*_{cb}V_{ud}\left[-\left(c_1 + \frac{c_2}{3}\right)F_{T\pi} - c_2 M'_{T\pi} + \left(c_1 + \frac{c_2}{3}\right)F_{A\pi} + c_2 M_{A\pi}\right], \tag{A4}$$

$$\mathcal{A}(B^0 \to D^{*0}K^0) = \frac{G_F}{\sqrt{2}} V^*_{ub}V_{cs}\left[\left(c_1 + \frac{c_2}{3}\right)F_{TK} + c_2 M_{TK}\right], \tag{A5}$$

$$\mathcal{A}(B^0 \to \bar{D}^{*0}K^0) = \frac{G_F}{\sqrt{2}} V^*_{cb}V_{us}\left[\left(c_1 + \frac{c_2}{3}\right)F_{TK} + c_2 M'_{TK}\right]; \tag{A6}$$

$$\mathcal{A}(B^+ \to D^{*+}\pi^0) = \frac{G_F}{2} V^*_{ub}V_{cd}\left[-\left(\frac{c_1}{3} + c_2\right)F_{AD^*} - c_1 M_{AD^*} + \left(\frac{c_1}{3} + c_2\right)F_{T\pi} + c_1 M_{T\pi}\right], \tag{A7}$$

$$\mathcal{A}(B^+ \to \bar{D}^{*0}\pi^+) = \frac{G_F}{\sqrt{2}} V^*_{cb} V_{ud} \left[\left(\frac{c_1}{3} + c_2\right) F_{TD^*} + c_1 M_{TD^*} + \left(c_1 + \frac{c_2}{3}\right) F_{T\pi} + c_2 M'_{T\pi} \right], \tag{A8}$$

$$\mathcal{A}(B^+ \to \bar{D}^{*0}K^+) = \frac{G_F}{\sqrt{2}} V^*_{cb} V_{us} \left[\left(\frac{c_1}{3} + c_2\right) F_{TD^*} + c_1 M_{TD^*} + \left(c_1 + \frac{c_2}{3}\right) F_{TK} + c_2 M'_{TK} \right], \tag{A9}$$

$$\mathcal{A}(B^+ \to D^{*0}K^+) = \frac{G_F}{\sqrt{2}} V^*_{ub} V_{cs} \left[\left(\frac{c_1}{3} + c_2\right) F_{AD^*} + c_1 M_{AD^*} + \left(c_1 + \frac{c_2}{3}\right) F_{TK} + c_2 M_{TK} \right]; \tag{A10}$$

$$\mathcal{A}(B^0_s \to D^{*-}_s \pi^+) = \frac{G_F}{\sqrt{2}} V^*_{cb} V_{ud} \left[\left(\frac{c_1}{3} + c_2\right) F_{TD^*_s} + c_1 M_{TD^*_s} \right], \tag{A11}$$

$$\mathcal{A}(B^0_s \to D^{*-}_s K^+) = \frac{G_F}{\sqrt{2}} V^*_{cb} V_{us} \left[\left(\frac{c_1}{3} + c_2\right) F_{TD^*_s} + c_1 M_{TD^*_s} + \left(c_1 + \frac{c_2}{3}\right) F_{AK} + c_2 M_{AK} \right], \tag{A12}$$

$$\mathcal{A}(B^0_s \to D^{*-}\pi^+) = \frac{G_F}{\sqrt{2}} V^*_{cb} V_{us} \left[\left(c_1 + \frac{c_2}{3}\right) F_{A\pi} + c_2 M_{A\pi} \right], \tag{A13}$$

$$\mathcal{A}(B^0_s \to D^{*+}K^-) = \frac{G_F}{\sqrt{2}} V^*_{ub} V_{cd} \left[\left(\frac{c_1}{3} + c_2\right) F_{TK} + c_1 M_{TK} \right], \tag{A14}$$

$$\mathcal{A}(B^0_s \to \bar{D}^{*0}\pi^0) = \frac{G_F}{2} V^*_{cb} V_{us} \left[\left(c_1 + \frac{c_2}{3}\right) F_{A\pi} + c_2 M_{A\pi} \right], \tag{A15}$$

$$\mathcal{A}(B^0_s \to \bar{D}^{*0}\bar{K}^0) = \frac{G_F}{\sqrt{2}} V^*_{cb} V_{ud} \left[\left(c_1 + \frac{c_2}{3}\right) F_{TK} + c_2 M'_{TK} \right], \tag{A16}$$

where $c_{i=1,2}(\mu)$ is the tree-level Wilson coefficients carrying the physics extending in the energy scale regions from m_W to m_B. The factorizable and nonfactorizable scattering amplitudes F and M carry the physics below the m_B energy scale; they are represented by means of the hadron matrix elements with four certified fermion effective operators, as expressed in Eq. (1). The pQCD calculation results in

$$F_{TD^*_{(s)}} = 8\pi C_F m_B^4 f_{\pi(K)} \int dx_1 dx_R \int b_1 db_1 b_R db_R \phi_B(x_1, b_1) \phi_{D\pi}(x_R, b_R, s)$$
$$\times \{[\sqrt{\zeta}(2x_R - 1) - x_R - 1] E_a^{(1)}(t_a) h_a(x_1, x_R, b_1, b_R) - (\zeta + r_c) E_a^{(2)}(t_b) h_b(x_1, x_R, b_1, b_R)\}, \tag{A17}$$

$$M_{TD^*_{(s)}} = 32\pi C_F m_B^4 / \sqrt{2N_c} \int dx_1 dx_R dx_3 \int b_1 db_1 b_3 db_3 \phi_B(x_1, b_1) \phi_{D\pi}(x_R, b_R, s) \phi^A$$
$$\times \{[\zeta(x_R - x_3 + 1) - x_R\sqrt{\zeta} + x_1 + x_3 - 1] E_b(t_c) h_c(x_1, x_R, x_3, b_1, b_3)$$
$$+ [x_3(1 - \zeta) + x_R(1 - \sqrt{\zeta}) - x_1] E_b(t_d) h_d(x_1, x_R, x_3, b_1, b_3)\}, \tag{A18}$$

$$F_{AD^*_{(s)}} = 8\pi C_F m_B^4 f_B \int dx_R dx_3 \int b_R db_R b_3 db_3 \phi_D(x_R, b_R, s)$$
$$\times \{[(1 - x_R)\phi^A + 2r_0 x_R \hat{\zeta} \sqrt{\zeta} \phi^P] E_c^{(1)}(t_e) h_e(x_R, x_3, b_R, b_3)$$
$$+ [(x_3(\zeta - 1) - \zeta)\phi^A - r_0 r_c [\phi^P + \hat{\zeta}(\zeta + 1)\phi^T]] E_c^{(2)}(t_f) h_f(x_R, x_3, b_R, b_3)\}, \tag{A19}$$

$$M_{AD^*_{(s)}} = 32\pi C_F m_B^4 / \sqrt{2N_c} \int dx_1 dx_R dx_3 \int b_1 db_1 b_R db_R \phi_B(x_1, b_1) \phi_{D\pi}(x_R, b_R, s)$$
$$\times \{[[\zeta(x_R + 1) + x_1 - x_3(\zeta - 1)]\phi^A + r_0\hat{\zeta} \sqrt{\zeta}[((1 - x_3)(1 - \zeta) - x_1)(\phi^P + \phi^T)$$
$$+ x_R(\phi^T - \phi^P)]] E_d(t_g) h_g(x_1, x_R, x_3, b_1, b_R) + [(1 - x_R)(\zeta - 1)\phi^A - r_0\hat{\zeta} \sqrt{\zeta}[(x_R - 1)(\phi^P + \phi^T)$$
$$+ (x_1 + x_3\zeta - \zeta - x_3)(\phi^T - \phi^P)]] E_d(t_h) h_h(x_1, x_R, x_3, b_1, b_R)\}; \tag{A20}$$

$$F_{T\pi(K)} = 8\pi C_F m_B^4 F_{D\pi}(s) \int dx_1 dx_3 \int b_1 db_1 b_3 db_3 \phi_B(x_1, b_1)$$

$$\times \{[\phi^A[x_3(1-\zeta)+1] - r_0[\phi^P(2x_3-1) + \phi^T\hat{\zeta}(2x_3(\zeta-1)+\zeta+1)]]E_e^{(1)}(t_m)$$

$$\times h_m(x_1, x_3, b_1, b_3) + [2r_0\hat{\zeta}\phi^P(\zeta(1-x_1)-1) - \zeta x_1 \phi^A]E_e^{(2)}(t_n)$$

$$\times h_n(x_1, x_3, b_1, b_3)\}, \tag{A21}$$

$$M_{T\pi(K)} = 32\pi C_F m_B^4/\sqrt{2N_c} \int dx_1 dx_R dx_3 \int b_1 db_1 b_R db_R \phi_B(x_1, b_1)\phi_{D\pi}(x_R, b_R, s)$$

$$\times \{[(\zeta-1)(1-x_1-x_R)\phi^A - r_0\hat{\zeta}[\zeta(x_R+x_1)(\phi^P+\phi^T) + x_3(1-\zeta)(\phi^P-\phi^T) - 2\zeta\phi^T]]$$

$$\times E_f(t_o)h_o(x_1, x_R, x_3, b_1, b_R) - [[r_c\sqrt{\zeta} + x_3(\zeta-1) - x_R + x_1]\phi^A + r_0\zeta(x_R-x_1)(\phi^T-\phi^P)$$

$$+ r_0[x_3(1-\zeta)\phi^P - (4r_c\sqrt{\zeta} + x_3\zeta - x_3)\phi^T]]E_f(t_p)h_p(x_1, x_R, x_3, b_1, b_R)\}, \tag{A22}$$

$$M'_{T\pi(K)} = 32\pi C_F m_B^4/\sqrt{2N_c} \int dx_1 dx_R dx_3 \int b_1 db_1 b_R db_R \phi_B(x_1, b_1)\phi_{D\pi}(x_R, b_R, s)$$

$$\times \{[\phi^A[x_1 + x_R - 1 - \sqrt{\zeta}r_c - \zeta(x_1+x_R-1)] - r_0\hat{\zeta}\zeta[\phi^P(x_1+x_R-x_3) + \phi^T(x_1+x_R+x_3-2)]$$

$$+ r_0 x_3\hat{\zeta}(\phi^T-\phi^P)]E_f(t_{o'})h_{o'}(x_1, x_R, x_3, b_1, b_R) - [[(\zeta-1)x_3 + x_1 - x_R]\phi^A + r_0 x_3(\phi^P+\phi^T)$$

$$+ r_0\zeta\hat{\zeta}(x_1-x_R)(\phi^T-\phi^P)]E_f(t_{p'})h_{p'}(x_1, x_R, x_3, b_1, b_R)\}, \tag{A23}$$

$$F_{AK} = 8\pi C_F m_B^4 f_B \int dx_R dx_3 \int b_R db_R b_3 db_3 \phi_{D\pi}(x_R, b_R, s))$$

$$\times \{[[((\zeta-1)x_3 + 1)\phi^A + r_0 r_c\phi^P] - r_0 r_c\hat{\zeta}(\zeta+1)\phi^T]E_g^{(1)}(t_s)h_s(x_R, x_3, b_R, b_3)$$

$$+ [-x_R\phi^A + 2r_0\hat{\zeta}\sqrt{\zeta}(\zeta+x_R-1)\phi^P]E_g^{(2)}(t_t)h_t(x_R, x_3, b_R, b_3)\}, \tag{A24}$$

$$M_{AK} = 32\pi C_F m_B^4/\sqrt{2N_c} \int dx_1 dx_R dx_3 \int b_1 db_1 b_3 db_3 \phi_B(x_1, b_1)\phi_{D\pi}(x_R, b_R, s)$$

$$\times \{[[(1-\zeta)(x_1+x_R) + \zeta]\phi^A - r_0\hat{\zeta}\sqrt{\zeta}[(x_3+\zeta+1-x_3\zeta)\phi^T + (1-\zeta)(x_3-1)\phi^P]$$

$$+ r_0\hat{\zeta}\sqrt{\zeta}(x_R+x_1)(\phi^T-\phi^P)]E_h(t_u)h_u(x_1, x_R, x_3, b_1, b_R) + [[\zeta(1+x_R-x_1-x_3) + x_3 - 1]\phi^A$$

$$+ r_0\sqrt{\zeta}[(x_3-1)(\phi^P-\phi^T) + \hat{\zeta}(x_1-x_R)(\phi^P+\phi^T)]]E_h(t_v)h_v(x_1, x_R, x_3, b_1, b_R)\}, \tag{A25}$$

with $\hat{\zeta} = 1/(\zeta - 1)$.

The hard scale t_i in the pQCD approach to deal with hard scatterings is chosen as the largest virtuality of the internal momentum transition,

$$t_a = \mathbf{Max}\{m_B\sqrt{|a_1|}, m_B\sqrt{|a_2|}, 1/b_R, 1/b_1\}, \quad t_b = \mathbf{Max}\{m_B\sqrt{|b_1|}, m_B\sqrt{|b_2|}, 1/b_1, 1/b_R\};$$

$$t_c = \mathbf{Max}\{m_B\sqrt{|c_1|}, m_B\sqrt{|c_2|}, 1/b_1, 1/b_3\}, \quad t_d = \mathbf{Max}\{m_B\sqrt{|d_1|}, m_B\sqrt{|d_2|}, 1/b_1, 1/b_3\};$$

$$t_e = \mathbf{Max}\{m_B\sqrt{|e_1|}, m_B\sqrt{|e_2|}, 1/b_R, 1/b_3\}, \quad t_f = \mathbf{Max}\{m_B\sqrt{|f_1|}, m_B\sqrt{|f_2|}, 1/b_3, 1/b_R\};$$

$$t_g = \mathbf{Max}\{m_B\sqrt{|g_1|}, m_B\sqrt{|g_2|}, 1/b_R, 1/b_1\}, \quad t_h = \mathbf{Max}\{m_B\sqrt{|h_1|}, m_B\sqrt{|h_2|}, 1/b_R, 1/b_1\};$$

$$t_m = \mathbf{Max}\{m_B\sqrt{|m_1|}, m_B\sqrt{|m_2|}, 1/b_3, 1/b_1\}, \quad t_n = \mathbf{Max}\{m_B\sqrt{|n_1|}, m_B\sqrt{|n_2|}, 1/b_1, 1/b_3\};$$

$$t_o = \mathbf{Max}\{m_B\sqrt{|o_1|}, m_B\sqrt{|o_2|}, 1/b_1, 1/b_R\}, \quad t_p = \mathbf{Max}\{m_B\sqrt{|p_1|}, m_B\sqrt{|p_2|}, 1/b_1, 1/b_R\};$$

$$t_{o'} = \mathbf{Max}\{m_B\sqrt{|o'_1|}, m_B\sqrt{|o'_2|}, 1/b_1, 1/b_R\}, \quad t_{p'} = \mathbf{Max}\{m_B\sqrt{|p'_1|}, m_B\sqrt{|p'_2|}, 1/b_1, 1/b_R\};$$

$$t_s = \mathbf{Max}\{m_B\sqrt{|s_1|}, m_B\sqrt{|s_2|}, 1/b_3, 1/b_R\}, \quad t_t = \mathbf{Max}\{m_B\sqrt{|t_1|}, m_B\sqrt{|t_2|}, 1/b_R, 1/b_3\};$$

$$t_u = \mathbf{Max}\{m_B\sqrt{|u_1|}, m_B\sqrt{|u_2|}, 1/b_R, 1/b_1\}, \quad t_v = \mathbf{Max}\{m_B\sqrt{|v_1|}, m_B\sqrt{|v_2|}, 1/b_R, 1/b_1\}. \tag{A26}$$

In the above expressions, the nondimensional kinematical factors are

$$
\begin{aligned}
&a_1 = x_R, &&a_2 = x_R x_1; \\
&b_1 = r_c^2 + x_1 - \zeta, &&b_2 = a_2; \\
&c_1 = a_2, &&c_2 = x_R[x_1 - (1-\zeta)(1-x_3)]; \\
&d_1 = a_2, &&d_2 = x_R[x_1 - (1-\zeta)x_3]; \\
&e_1 = x_R - 1, &&e_2 = (1-x_R)[x_3(\zeta-1) - \zeta]; \\
&f_1 = r_c^2 + x_3(\zeta-1) - \zeta, &&f_2 = e_2; \\
&g_1 = e_2, &&g_2 = x_R[x_1 + (x_3-1)(1-\zeta)] + 1; \\
&h_1 = e_2, &&h_2 = (1-x_R)(x_1 + x_3\zeta - x_3 - \zeta); \\
&m_1 = (1-\zeta)x_3, &&m_2 = (1-\zeta)x_3 x_1; \\
&n_1 = (1-\zeta)x_1, &&n_2 = m_2; \\
&o_1 = m_2, &&o_2 = (1 - x_1 - x_R)(x_3\zeta - x_3 - \zeta); \\
&p_1 = m_2, &&p_2 = r_c^2 + x_3(\zeta-1)(x_R - x_1); \\
&o'_1 = (1-\zeta)x_3 x_1, &&o'_2 = r_c^2 - (x_R + x_1 - 1)(x_3(\zeta-1) - \zeta); \\
&p'_1 = o'_1, &&p'_2 = x_3(\zeta-1)(x_R - x_1); \\
&s_1 = r_c^2 - x_3\zeta + x_3 - 1, &&s_2 = x_R(x_3-1)(1-\zeta); \\
&t_1 = x_R(\zeta-1), &&t_2 = s_2; \\
&u_1 = s_2, &&u_2 = (x_R + x_1 - 1)(\zeta + x_3 - x_3\zeta) + 1; \\
&v_1 = s_2, &&v_2 = (x_3-1)(1-\zeta)(x_R - x_1).
\end{aligned}
\tag{A27}
$$

The hard functions h_i ($i \in \{a,b,c,d,e,f,g,h,m,n,o,p,o',p',s,t,u,v\}$) in scattering amplitudes is expressed in terms of transversal distances b_i conjugated to the transversal momentum by a Fourier transform.

$$
h_i(x1, x2, (x3), b_1, b_2) = h_{i1}(\beta, b_2) \times h_{i2}(\alpha, b_1, b_2),
$$

$$
h_{i1}(\beta, b_2) = \begin{cases} K_0(\sqrt{\beta}b_2), & \beta > 0 \\ \frac{i\pi}{2} H_0^{(1)}(\sqrt{-\beta}b_2), & \beta < 0 \end{cases}
$$

$$
h_{i2}(\alpha, b_1, b_2) = \begin{cases} \theta(b_2 - b_1)I_0(\sqrt{\alpha}b_1)K_0(\sqrt{\alpha}b_2) + (b_1 \leftrightarrow b_2), & \alpha > 0 \\ \frac{i\pi}{2}\theta(b_2 - b_1)J_0(\sqrt{-\alpha}b_1)H_0^{(1)}(\sqrt{-\alpha}b_2) + (b_1 \leftrightarrow b_2), & \alpha < 0 \end{cases}
\tag{A28}
$$

where J_0 is the Bessel function, K_0 and I_0 are modified Bessel functions, N_0 is the Neumann function, and H_0 is the Hankel function of the first kind with relation $H_0^{(1)}(x) = J_0(x) + iN_0(x)$. The kinematic factors α and β are exactly the certain case of i_1 and i_2 defined in Eq. (A27), respectively.

The evolution functions in the scattering amplitudes take into account the strong coupling constant and also the Sudakov suppressed factors from the resummations of end point singularity [4,5],

$$
E_a^{(1)}(t) = \alpha_s(t)\exp[-S_B(t) - S_C(t)]S_t(x_R),
$$

$$
E_a^{(2)}(t) = \alpha_s(t)\exp[-S_B(t) - S_C(t)]S_t(x_1),
\tag{A29}
$$

$$
E_b(t) = \alpha_s(t)\exp[-S_B(t) - S_C(t) - S_P(t)]|_{b_R = b_1},
\tag{A30}
$$

$$
E_c^{(1)}(t) = \alpha_s(t)\exp[-S_C(t) - S_P(t)]S_t(x_R),
$$

$$
E_c^{(2)}(t) = \alpha_s(t)\exp[-S_C(t) - S_P(t)]S_t(x_3),
\tag{A31}
$$

$$
E_d(t) = \alpha_s(t)\exp[-S_B(t) - S_C(t) - S_P(t)]|_{b_3 = b_R},
\tag{A32}
$$

$$
E_e^{(1)}(t) = \alpha_s(t)\exp[-S_B(t) - S_P(t)]S_t(x_3),
$$

$$
E_e^{(2)}(t) = \alpha_s(t)\exp[-S_B(t) - S_P(t)]S_t(x_1),
\tag{A33}
$$

$$
E_f(t) = \alpha_s(t)\exp[-S_B(t) - S_C(t) - S_P(t)]|_{b_3 = b_1},
\tag{A34}
$$

$$E_g^{(1)}(t) = \alpha_s(t) \exp[-S_C(t) - S_P(t)]S_t(x_3),$$

$$E_g^{(2)}(t) = \alpha_s(t) \exp[-S_C(t) - S_P(t)]S_t(x_R), \tag{A35}$$

$$E_h(t) = \alpha_s(t) \exp[-S_B(t) - S_C(t) - S_P(t)]|_{b_3=b_R}. \tag{A36}$$

APPENDIX B: THE $D_{(s)}h$ FORM FACTOR UNDER THE $D_{(s)}^*$ DOMINANT APPROXIMATION

The timelike $D_{(s)}h$ form factor is defined by the transition matrix element from a vacuum to the $D_{(s)}h$ system sandwiched by a weak current,

$$\langle D_{(s)}h|\bar{c}\gamma_\mu(1-\gamma_5)q|0\rangle = -\left(\bar{p}_{R\mu} - \frac{m_{D_{(s)}}^2 - m_h^2}{s}p_{R\mu}\right)F_{D_{(s)}h}^V(s) - \frac{m_{D_{(s)}}^2 - m_h^2}{s}p_{R\mu}F_{D_{(s)}h}^S(s), \tag{B1}$$

in which the on shell conditions of the final mesons $p_{D_{(s)}}^2 = m_{D_{(s)}}^2$ and $p_h^2 = m_h^2$ are indicated. Multiplying both sides by $\bar{p}_R^\mu$, it modifies to

$$\bar{p}_R^\mu\langle D_{(s)}h|\bar{c}\gamma_\mu(1-\gamma_5)q|0\rangle = -\frac{1}{s}[2(m_{D_{(s)}}^2 + m_h^2)s - s^2 - (m_{D_{(s)}}^2 - m_h^2)^2]F_{D_{(s)}h}^V(s). \tag{B2}$$

We note that the scalar form factor term is neglected here since the involved $D_{(s)}h$ system is in the P-wave component. In the singe resonance $D_{(s)}^*$ approximation, the matrix element from a vacuum to the $D_{(s)}h$ system is detached to

$$\langle D_{(s)}h|\bar{c}\gamma_\mu(1-\gamma_5)q|0\rangle \rightarrow \frac{\langle D_{(s)}h|D_{(s)}^*\rangle\langle D_{(s)}^*|\bar{c}\gamma_\mu(1-\gamma_5)q|0\rangle}{[m_{D_{(s)}}^2 - s - im_{D_{(s)}^*}\Gamma_{D_{(s)}^*}(s)]} = \frac{\sqrt{s}g_{D_{(s)}^*D_{(s)}h}f_{D_{(s)}^*}\sum_{\mu,\nu}\epsilon_\mu^*\epsilon_\nu\bar{p}_{D_{(s)}^*}^\nu}{[m_{D_{(s)}}^2 - s - im_{D_{(s)}^*}\Gamma_{D_{(s)}^*}(s)]}. \tag{B3}$$

To obtain this expression, the definitions $\langle D_{(s)}h|D_{(s)}^*\rangle = g_{D_{(s)}^*D_{(s)}h}(\bar{p}_{D_{(s)}}^* \cdot \epsilon)$ and $\langle D_{(s)}^*|\bar{c}\gamma_\mu(1-\gamma_5)q|0\rangle = f_{D_{(s)}^*}|p_{D_{(s)}^*}|\epsilon_\mu^*$ are used. Substituting Eq. (B3) in to Eq. (B2), we obtain the timelike $D_{(s)}h$ form factor in Eq. (13).

[1] E. Kou *et al.* (Belle-II Collaboration), Prog. Theor. Exp. Phys. (**2019**), 123C01; (**2020**), 029201(E).

[2] R. Aaij *et al.* (LHCb Collaboration), Phys. Rev. Lett. **111**, 101801 (2013).

[3] Y. Y. Keum, H. n. Li, and A. I. Sanda, Phys. Lett. B **504**, 6 (2001).

[4] Y. Y. Keum, H. N. Li, and A. I. Sanda, Phys. Rev. D **63**, 054008 (2001).

[5] C. D. Lu, K. Ukai, and M. Z. Yang, Phys. Rev. D **63**, 074009 (2001).

[6] H. n. Li, Prog. Part. Nucl. Phys. **51**, 85 (2003).

[7] M. Beneke, G. Buchalla, M. Neubert, and C. T. Sachrajda, Phys. Rev. Lett. **83**, 1914 (1999).

[8] M. Beneke, G. Buchalla, M. Neubert, and C. T. Sachrajda, Nucl. Phys. **B591**, 313 (2000).

[9] M. Beneke, G. Buchalla, M. Neubert, and C. T. Sachrajda, Nucl. Phys. **B606**, 245 (2001).

[10] M. Beneke and M. Neubert, Nucl. Phys. **B675**, 333 (2003).

[11] C. H. Chen and H. n. Li, Phys. Lett. B **561**, 258 (2003).

[12] W. F. Wang, H. C. Hu, H. n. Li, and C. D. Lü, Phys. Rev. D **89**, 074031 (2014).

[13] W. F. Wang, H. n. Li, W. Wang, and C. D. Lü, Phys. Rev. D **91**, 094024 (2015).

[14] A. J. Ma, Y. Li, W. F. Wang, and Z. J. Xiao, Nucl. Phys. **B923**, 54 (2017).

[15] S. Kränkl, T. Mannel, and J. Virto, Nucl. Phys. **B899**, 247 (2015).

[16] T. Mannel, K. Olschewsky, and K. K. Vos, J. High Energy Phys. 06 (2020) 073.

[17] T. Huber, J. Virto, and K. K. Vos, J. High Energy Phys. 11 (2020) 103.

[18] H. Y. Cheng and C. K. Chua, Phys. Rev. D **88**, 114014 (2013).

[19] H. Y. Cheng and C. K. Chua, Phys. Rev. D **89**, 074025 (2014).

[20] H. Y. Cheng and C. K. Chua, Phys. Rev. D **102**, 053006 (2020).

[21] Z. H. Zhang, X. H. Guo, and Y. D. Yang, Phys. Rev. D **87**, 076007 (2013).

[22] C. Wang, Z. H. Zhang, Z. Y. Wang, and X. H. Guo, Eur. Phys. J. C **75**, 536 (2015).

[23] A. Furman, R. Kaminski, L. Lesniak, and P. Zenczykowski, Phys. Lett. B **699**, 102 (2011).

[24] B. El-Bennich, A. Furman, R. Kaminski, L. Lesniak, B. Loiseau, and B. Moussallam, Phys. Rev. D **79**, 094005 (2009); **83**, 039903(E) (2011).

[25] M. Gronau and J. L. Rosner, Phys. Rev. D **72**, 094031 (2005).

[26] D. Xu, G. N. Li, and X. G. He, Phys. Lett. B **728**, 579 (2014).

[27] G. Engelhard, Y. Nir, and G. Raz, Phys. Rev. D **72**, 075013 (2005).

[28] M. Imbeault and D. London, Phys. Rev. D **84**, 056002 (2011).

[29] B. Bhattacharya, M. Gronau, and J. L. Rosner, Phys. Lett. B **726**, 337 (2013).

[30] B. Bhattacharya, M. Gronau, M. Imbeault, D. London, and J. L. Rosner, Phys. Rev. D **89**, 074043 (2014).

[31] H. n. Li and B. Melic, Eur. Phys. J. C **11**, 695 (1999).

[32] T. Kurimoto, H. n. Li, and A. I. Sanda, Phys. Rev. D **67**, 054028 (2003).

[33] C. Y. Wu, T. W. Yeh, and H. n. Li, Phys. Rev. D **53**, 4982 (1996).

[34] C. Y. Wu, T. W. Yeh, and H. n. Li, Phys. Rev. D **55**, 237 (1997).

[35] Y. Y. Keum, T. Kurimoto, H. N. Li, C. D. Lu, and A. I. Sanda, Phys. Rev. D **69**, 094018 (2004).

[36] H. Y. Cheng and B. Tseng, Phys. Rev. D **51**, 6259 (1995).

[37] Y. S. Amhis *et al.* (HFLAV Collaboration), arXiv:1909.12524.

[38] S. H. Zhou, Y. B. Wei, Q. Qin, Y. Li, F. S. Yu, and C. D. Lu, Phys. Rev. D **92**, 094016 (2015).

[39] K. Azizi, R. Khosravi, and F. Falahati, Int. J. Mod. Phys. A **24**, 5845 (2009).

[40] Y. Li and C. D. Lu, J. Phys. G **29**, 2115 (2003).

[41] R. H. Li, C. D. Lu, and H. Zou, Phys. Rev. D **78**, 014018 (2008).

[42] H. Zou, R. H. Li, X. X. Wang, and C. D. Lu, J. Phys. G **37**, 015002 (2010).

[43] K. Abe *et al.* (Belle Collaboration), Phys. Rev. D **69**, 112002 (2004).

[44] A. Kuzmin *et al.* (Belle Collaboration), Phys. Rev. D **76**, 012006 (2007).

[45] B. Aubert *et al.* (*BABAR* Collaboration), Phys. Rev. D **79**, 112004 (2009).

[46] B. Aubert *et al.* (*BABAR* Collaboration), Phys. Rev. Lett. **100**, 171803 (2008).

[47] J. Wiechczynski *et al.* (Belle Collaboration), Phys. Rev. D **91**, 032008 (2015).

[48] R. Aaij *et al.* (LHCb Collaboration), Phys. Rev. D **90**, 072003 (2014).

[49] R. Aaij *et al.* (LHCb Collaboration), Phys. Rev. D **91**, 092002 (2015); **93**, 119901(E) (2016).

[50] R. Aaij *et al.* (LHCb Collaboration), Phys. Rev. D **92**, 012012 (2015).

[51] R. Aaij *et al.* (LHCb Collaboration), Phys. Rev. D **92**, 032002 (2015).

[52] R. Aaij *et al.* (LHCb Collaboration), Phys. Rev. D **94**, 072001 (2016).

[53] W. F. Wang, Phys. Rev. D **101**, 111901(R) (2020); **103**, 056021(E) (2021).

[54] A. Le Yaouanc, J. P. Leroy, and P. Roudeau, Phys. Rev. D **99**, 073010 (2019).

[55] W. F. Wang and J. Chai, Phys. Lett. B **791**, 342 (2019).

[56] G. Buchalla, A. J. Buras, and M. E. Lautenbacher, Rev. Mod. Phys. **68**, 1125 (1996).

[57] A. G. Grozin and M. Neubert, Phys. Rev. D **55**, 272 (1997).

[58] T. Kurimoto, H. n. Li, and A. I. Sanda, Phys. Rev. D **65**, 014007 (2001).

[59] V. M. Braun, Y. Ji, and A. N. Manashov, J. High Energy Phys. 05 (2017) 022.

[60] M. Beneke, V. M. Braun, Y. Ji, and Y. B. Wei, J. High Energy Phys. 07 (2018) 154.

[61] P. Ball, V. M. Braun, and A. Lenz, J. High Energy Phys. 05 (2006) 004.

[62] S. Cheng, Phys. Rev. D **100**, 013007 (2019).

[63] J. P. Lees *et al.* (*BABAR* Collaboration), Phys. Rev. D **88**, 052003 (2013); **88**, 079902(E) (2013).

[64] J. P. Lees *et al.* (*BABAR* Collaboration), Phys. Rev. Lett. **111**, 111801 (2013).

[65] P. Colangelo and F. De Fazio, Phys. Lett. B **532**, 193 (2002).

[66] Z. G. Wang and S. L. Wan, Phys. Rev. D **74**, 014017 (2006).

[67] A. Anastassov *et al.* (CLEO Collaboration), Phys. Rev. D **65**, 032003 (2002).

[68] D. Becirevic and A. Le Yaouanc, J. High Energy Phys. 03 (1999) 021.

[69] J. Blatt and V. E. Weisskopf, *Theoretical Nuclear Physics* (Wiley, New York, 1952).

[70] B. Aubert *et al.* (*BABAR* Collaboration), Phys. Rev. D **72**, 072003 (2005); **74**, 099903(E) (2006).

[71] P. A. Zyla *et al.* (Particle Data Group), Prog. Theor. Exp. Phys. (**2020**), 083C01.

[72] G. C. Donald, C. T. H. Davies, J. Koponen, and G. P. Lepage, Phys. Rev. Lett. **112**, 212002 (2014).

[73] G. L. Yu, Z. Y. Li, and Z. G. Wang, Eur. Phys. J. C **75**, 243 (2015).

[74] B. Yang, B. Wang, L. Meng, and S. L. Zhu, Phys. Rev. D **101**, 054019 (2020).

[75] F. K. Guo, Phys. Rev. Lett. **122**, 202002 (2019).

[76] S. Narison, Int. J. Mod. Phys. A **30**, 1550116 (2015); Nucl. Part. Phys. Proc. **270-272**, 143 (2016).

[77] A. Bazavov, C. Bernard, N. Brown, C. Detar, A. X. El-Khadra, E. Gámiz, S. Gottlieb, U. M. Heller, J. Komijani, and A. S. Kronfeld *et al.*, Phys. Rev. D **98**, 074512 (2018).

[78] A. Ali, G. Kramer, Y. Li, C. D. Lu, Y. L. Shen, W. Wang, and Y. M. Wang, Phys. Rev. D **76**, 074018 (2007).